

On-orbit performance testing of the Pointing Calibration & Reference Sensor for the Spitzer Space Telescope

Amanda K. Mainzer^{*a}, Erick T. Young^b, Daniel S. Swanson^c.

^a Jet Propulsion Laboratory, 4800 Oak Grove Dr., Pasadena, CA 91109;

^b Steward Observatory, University of Arizona, Tucson, AZ 85721;

^c Lockheed Martin Space Systems Company, Sunnyvale, CA 94089

ABSTRACT

We present the on-orbit performance results of the Pointing Calibration and Reference Sensor (PCRS) for the Spitzer Space Telescope. A cryogenic optical (center wavelength 0.55 μm) imager, the PCRS serves as the Observatory's fine guidance sensor by providing an alignment reference between the telescope boresight and the external spacecraft attitude determination system. The PCRS makes precision measurements of the positions of known guide stars; these are used to calibrate measurements from Spitzer's star tracker and gyroscopes to obtain the actual pointing of the Spitzer telescope. The PCRS calibrates out thermomechanical drifts between the 300 K spacecraft bus and the 5.5 K telescope. By using only 16 pixels, the PCRS provides high precision centroiding with extremely low ($\sim 64 \mu\text{W}$) power dissipation, resulting in minimal impact to Spitzer's helium lifetime. We have demonstrated that the PCRS meets its centroiding accuracy requirement of 0.14 arcsec 1- σ radial, which represents $\sim 1/100$ pixel centroiding. The Spitzer Space Telescope was launched on 25 August, 2003 and completed its In-Orbit Checkout phase two months later; the PCRS has been operating failure-free ever since.

Keywords: infrared, cryogenic, optical, telescope, SIRTf, Spitzer, guidance, centroiding, pointing

1. INTRODUCTION

The Pointing Calibration and Reference Sensor (PCRS) is a cryogenic instrument with a center wavelength of 0.55 μm collocated with the Spitzer Space Telescope science instruments inside the Multiple Instrument Chamber (MIC). It serves as the Observatory's fine guidance sensor by providing an alignment reference between the telescope boresight and the external spacecraft attitude determination system¹. The PCRS makes precision measurements of the positions of known guide stars with an accuracy of 0.14 arcsec 1- σ radial; these are compared with measurements from Spitzer's

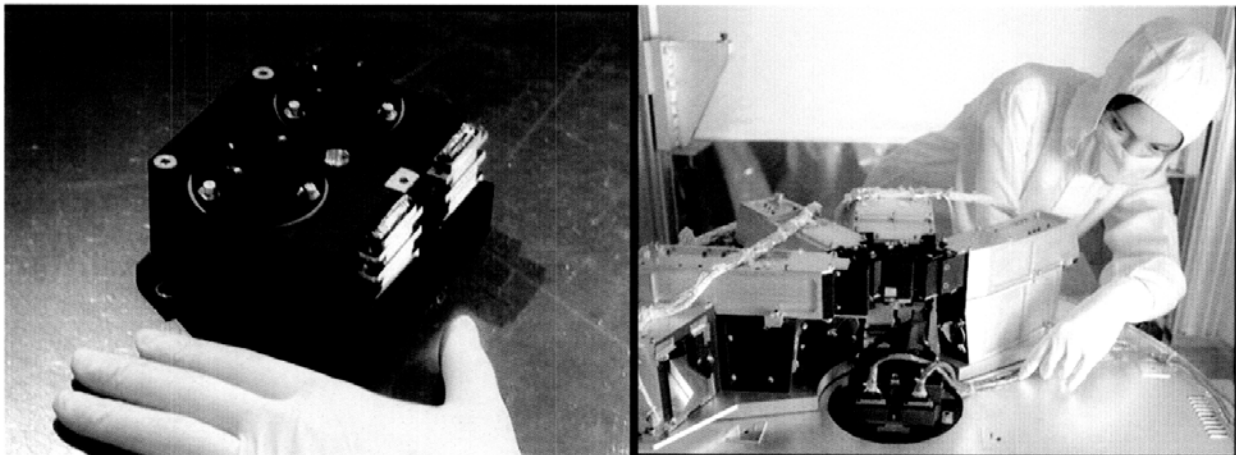


Figure 1a: The Flight Cold Assembly, on the bench and during its installation into the Multiple Instrument Chamber.

star trackers and gyroscopes to obtain the actual pointing of the Spitzer telescope. This procedure calibrates out thermomechanical drifts between the 300 K spacecraft bus and the 5.5 K telescope. Currently, we estimate that we must perform this thermomechanical drift calibration once every twelve hours.²

The PCRS also calibrates out uncertainty in the roll angle about the telescope boresight axis. We have two separate PCRS apertures located symmetrically about the Spitzer coordinate origin. To measure the roll angle, we first capture a star in one aperture, then scan the star over to where we think the other aperture is. The difference between where the star lands on the second array and the array center defines the roll angle error, which is then calibrated out.

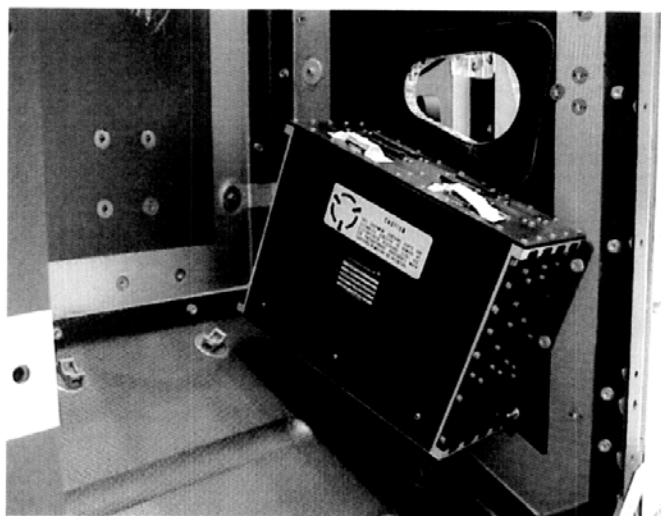


Figure 1b: The PCRS Warm Electronics being fit-checked in the spacecraft bus.

The third usage of the PCRS is to initialize the pointing system for science observations that require high precision attitude knowledge. For example, the Infrared Spectrograph (IRS) requires accurate placement of the target in a spectrometer slit. The PCRS can be used to first peak up the guidance system on a known visible star and then precisely offset the pointing to place the infrared target in the spectrograph. This peakup capability is available to Spitzer observers as an alternative to the IRS peakup mode.

Even though the PCRS most resembles the science instruments, it is an integral part of the Observatory's pointing control system. The

instrument consists of a Cold Assembly (CA) and Warm Electronics (WE). The Cold Assembly (see Fig. 1a), which resides in the 1.4 K Multiple Instrument Chamber, contains relay optics, filters, detector arrays, and cryogenic readout/multiplexers. Hence, even though the PCRS most resembles the science instruments, it is an integral part of the Observatory's pointing control system. The Cold Assembly contains four 4x4-pixel silicon PIN detector arrays, along with supporting readout electronics, relay optics, and filters. Two of the arrays serve as the primary boresight alignment redundant, so the Cold Assembly contains two totally independent electrical halves, from the detectors to the readouts, ceramic fanout board traces, cables, and connectors. Thus, there are four PCRS arrays: Array 1A and 2A (the 1 and 2 refer to "central" and "roll" arrays; the A refers to the redundant optical side) and 1B and 2B (the redundant roll and central arrays, which are currently powered off and will remain so unless the A side becomes nonfunctional). The Cold Assembly sits on the bottom of the Multiple Instrument Chamber, underneath the pickoff mirrors of the other science instruments. Since space limitations prevented the placement of the PCRS detectors in the Spitzer focal surface, relay optics were required to transfer the image down to the PCRS focal plane arrays. Each redundant PCRS focal plane array contains two 4x4 silicon PIN detectors, manufactured by United Detector Technology of Hawthorne CA, which are read out and controlled using the CRC-696 32 channel cryogenic multiplexer developed under NASA support at the Hughes Technology Center (now Raytheon Infrared Center of Excellence).³ The CRC-696 devices operate well at the Spitzer focal plane temperatures, and were originally designed for the Ge:Ga far infrared focal plane arrays used on the Multiband Imaging Photometer for Spitzer (MIPS). The silicon PIN diodes were specially selected and fabricated to operate well at the 1.4 K operating temperature of the MIC.

The Warm Electronics (see Fig 1b), installed in the ~300 K spacecraft bus, supplies the voltages and currents necessary to power the Cold Assembly, along with the A/D converters, power supply boards, and FPGAs required to digitize the data and perform preliminary processing on it before sending it to the main spacecraft computer. The Warm Electronics clock is synchronized to the main spacecraft clock to provide accurate time stamping, allowing us to compute PCRS star centroids that can be compared directly to the star tracker/gyro outputs. Table 1 summarizes the general instrument characteristics. A detailed description of the PCRS can be found in Mainzer et al. 2003.

Characteristic	Value
center wavelength	550 nm
filter bandpass	520-600 nm; defined by Schott BG39 + OG515 Filters

magnitude range	V= 7 – 10
detector type	Silicon PIN
detector format	Four arrays of 4x4 pixels
array operating temperature	1.1 – 1.5 K
readout type	Raytheon CRC-696
pixel size	250 x 250 μm
array field of view	40x40 arcsec
read noise	118 electrons
well depth	250,000 electrons
dark current	< 0.1 electron/sec
integration time	0.5 – 25.5 sec
centroiding accuracy in “sweetspot” region	0.14 arcsec 1- σ radial
centroiding accuracy outside “sweetspot” region	0.5 arcsec 1- σ radial
radius of “sweetspot”	2 arcsec

Table 1: PCRS general characteristics.

2. SOFTWARE DESIGN

2.1. Centroiding Performance

Although it has only 16 pixels, each 10 arcsec across, the PCRS is still able to achieve a centroiding accuracy of 0.1 arcsec 1- σ per axis. This accuracy, better than 1/100 of a pixel, is accomplished by making a high resolution map of the sub-pixel responses and matching the responses coming out of the central four pixels to the map. We only use the inner ± 2 arcsec of each array as the calibrated region in which high precision centroiding is available (the “sweetspot”).

The centroiding algorithm, which was custom written for this application, uses a modified Newton’s method routine to match the signals coming out of the four inner pixels to the four pixel response maps. Before launch, we generated the sub-pixel response maps for each array by raster scanning a simulated star across each pixel with fine steps. The resulting grid of data was fitted to a set of Chebyshev polynomials. We chose Chebyshev polynomials because they decrease with each successive coefficient, allowing us to gracefully truncate them to save space and increase processing speed. The algorithm minimizes the χ^2 derived from comparing the four pixels’ measured values to the pixel response map, which is now represented by the Chebyshev polynomials. The algorithm computes the centroid fast enough to be run each time the detector collects an image. After any cosmic rays have been removed from the data, the resulting set of centroids are then averaged together to provide a final star position. These calibration grids had to be regenerated after launch as described in Section 3 below.

By defocusing the highly irregular non-diffraction limited image from the telescope, we smoothed out the PCRS’s point spread function (PSF). See Figure 2. This resulted in a much more uniform sub-pixel response, which allowed us to centroid with greater precision using fewer mapping points than if the PSF exhibited great variability across each pixel. By performing a series of discrete offsets across the array using a high precision translation stage to move the simulated star, we assessed how well the centroiding algorithm works. These tests yielded an average accuracy better than the required 0.1 arcsec 1- σ per axis. We therefore concluded that the PCRS would meet its accuracy requirement in the calibrated region. A similar accuracy test designed to take advantage of Spitzer’s precision maneuvering capability was performed on orbit, as described in Section 3 below.

The remainder of the inner four pixels, plus the outer 12 pixels, were used strictly for initial acquisition purposes. The measured centroiding error for these outer parts of the array is approximately 0.5 arcsec 1- σ radial. This result accords well with what one would expect for typical centroiding performance resulting from a simple weighted-average centroid equation. Here, the accuracy was measured to be 1/10-1/20 of a pixel, or 0.5 – 1 arcsec centroiding accuracy. During nominal operations, Spitzer’s blind pointing capability has been measured to be sufficiently good to reduce the chances of landing outside the inner four pixels to essentially zero. At this juncture, the outer 12 pixels are never used.

2.2. PCRS Guide Star Catalog

In order to provide 0.14 arcsec centroiding accuracy, a source catalog with positional error no greater than 0.05 arcsec over the entire mission duration had to be created: the PCRS Guide Star Catalog. To avoid buildup of gyroscopic drift errors, the pointing control system is required to slew no more than 30 arcmin between guide stars. This sets the mean separation between stars in the PCRS Guide Star Catalog and therefore the total catalog size. With only 16 pixels, the PCRS cannot distinguish between single and multiple stars. Since a close neighbor would result in a shifted centroid measurement, a strict no-neighbors requirement was levied against potential catalog sources. The guide stars, which need to have a magnitude between 7 and 10 in the V band, were initially selected using the Tycho-1, Tycho-2, and Hipparcos catalogs. In order to obtain sufficient depth, the 2MASS point source catalog was used to compute the disturbing effect of nearby stars. Local star number density, derived from the USNO A2 catalog, was utilized to compensate for “blind areas” around the (bright) guide star candidates. The celestial background level and slope at the guide star candidate locations were provided by the digitized sky survey (DSS) catalog. Finally, the disturbing effect of approximately 1.9 million extended objects obtained from the 2MASS extended source catalog and the HyperLeda database was computed to arrive at the final catalog of 196,087 PCRS guide stars.⁴ The PCRS Guide Star Catalog has been made available for general Spitzer observers to use when planning IRS observations.

3. ORBITAL OPERATIONS

3.1. In-Orbit Checkout (IOC)

The PCRS had numerous calibration sequences that were performed during the 60 day In-Orbit Checkout (IOC) phase immediately following launch. These included tests to verify focus, photometric response, radiation response, system noise performance, stray light performance, the calibration of the pixel response coefficients, spacecraft jitter, and centroiding accuracy.

3.1.1. System Noise

System noise was assessed initially by integrating for 15 minutes prior to dust cover ejection. Noise performance was compared to pre-launch levels and was found to be substantially better than the quietest environment ever achieved on the ground. The rms dark noise was measured to be ~10 dN/sec, or 70 electrons/sec.

3.1.2. Spitzer First Light

The PCRS was the first instrument to see light on board Spitzer. The instrument was first powered on three days after

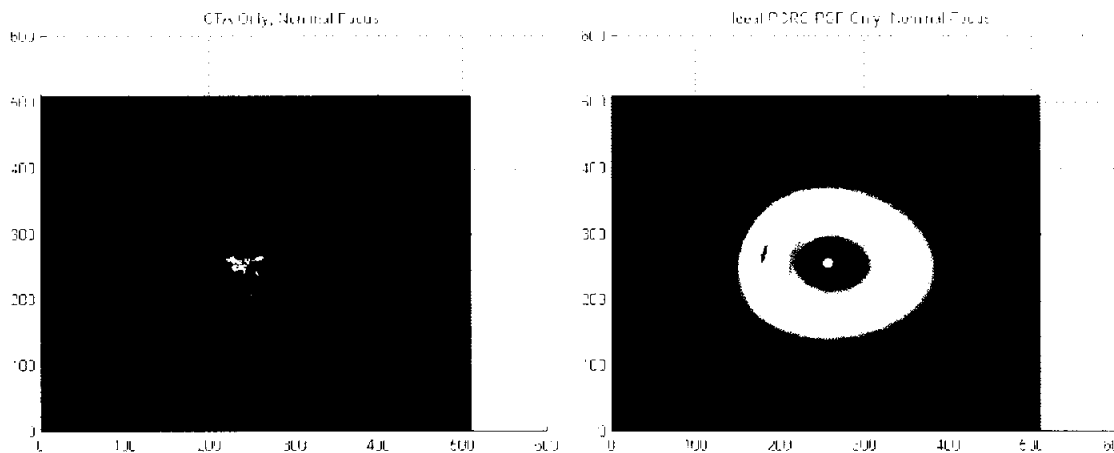


Figure 2: PCRS model point spread functions both with and without the defocus. The PSF without defocus is irregular since it is operating at 0.55 μm , well below the SIRTf 3 μm diffraction limit.

launch prior to dust cover ejection in order to collect dark frames which were used to assess system noise performance. First light was achieved 5 days after launch following dust cover ejection and aperture door opening. The purpose of this measurement was simply to verify that the dust cover and aperture door were both open. Since the telescope

boresight angle relative to the star tracker was poorly known at this point (~ 30 arcmin), we pointed the PCRS at the rich open cluster M7. This resulted in a high probability of landing on a star. Indeed, we successfully captured a star in the Array 2 field of view.

3.1.3. Initial PCRS Acquisition

Nine days after launch, the uncertainty in the location of the PCRS arrays was still approximately 30 arcmin. Thus, we needed to use all 16 pixels to locate the array to improve the chances of finding the array. Since each pixel subtends ~ 10 arcsec, using the full 4×4 array gave us a 40×40 arcsec target. Initial acquisition was accomplished by rastering Array 1 across a 1° square area. The target star was chosen to be free of nearby neighbors bright enough to be detectable by the PCRS; the detection threshold was set such that the target star triggered the Observatory to stop when it was encountered. Once Array 1 was located, Array 2 was located by executing a smaller raster pattern based on the uncertainty in the roll angle.

3.1.4. Photometric Response

The photometric response of the PCRS to stars of well-known magnitudes was established shortly after initial PCRS acquisition, allowing us to confirm exposure times. Four stars of known magnitudes ranging from 7 – 10, plus one third magnitude star, were selected within Spitzer’s continuous viewing zone (CVZ) to be observed by PCRS with varying exposure times. By selecting stars within the CVZ, we can go back and reobserve them periodically to verify that the instrument’s photometric response has not changed over time, particularly as radiation dose is accumulated. Typical exposure times range from 0.5 – 1.0 sec per frame; typically, 30 frames are collected.

3.1.5. Focus

The PCRS is mounted with the Spitzer science instruments inside the MIC and shares part of the Spitzer focal surface. It must therefore be compatible with the focus chosen for the Infrared Array Camera (IRAC), the Infrared Spectrograph (IRS), and the Multiband Imaging Photometer for SIRTf (MIPS). The Spitzer pointing control system was required to point to any location on the sky with an accuracy of 5 arcsec $1-\sigma$ radial. This means that we were required to land a star within 5 arcsec of the PCRS array centers 67% of the time. We therefore sized the calibrated region of the PCRS, the sweetspot, to accommodate this range. In order to provide a suitably large target image for the Spitzer attitude control system, the PCRS was deliberately defocused by 4.40 mm relative to best focus as defined by the IRAC instrument. This expanded the PCRS image from ~ 1.5 arcsec diameter at the PCRS best focus to ~ 6.5 arcsec diameter at the IRAC best focus. The other reason for deliberately defocusing the PCRS is that although the Spitzer telescope is diffraction limited at $6 \mu\text{m}$, the PCRS must operate at $0.55 \mu\text{m}$ in order to use existing high precision star catalogs. At visible wavelengths, irregularities in the Spitzer optics scatter light and produce a PSF much larger than

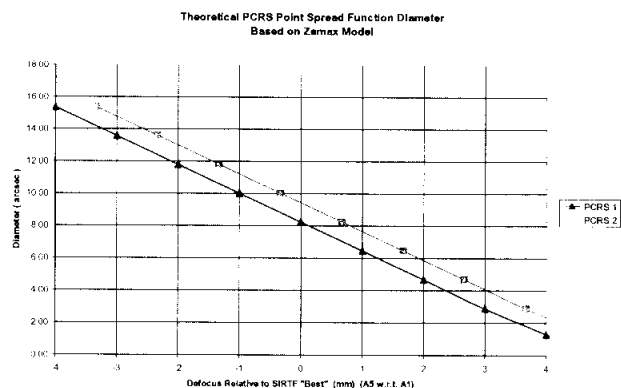


Figure 3: PCRS image diameter as a function of telescope focus.

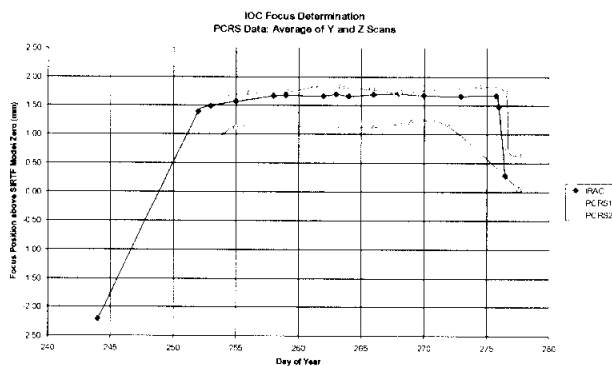


Figure 4: PCRS focus for Arrays 1 and 2 as a function of time during the Spitzer In-Orbit Checkout phase; the telescope is steadily dropping in temperature from 300 K down to 5.5 K. The blue points represent focus measurements made by the IRAC instrument.

the diffraction limit. Thus, by deliberately defocusing the PCRS, we have smoothed out the extremely irregular point spread function from the telescope and PCRS alone. Figure 2 shows the model point spread functions resulting from the Spitzer telescope and PCRS with and without defocus. Changing the focus results in a linear growth in the PCRS' image diameter; 1 mm of defocus results in approximately 1 arcsec diameter change. The PCRS contains four redundant 4x4 arrays with 10 arcsec pixels. With only 16 pixels, the PCRS cannot adequately sample its point spread function by imaging alone. Hence, the image diameter must be measured by scanning a star across the array and seeing when the image crosses each pixel.

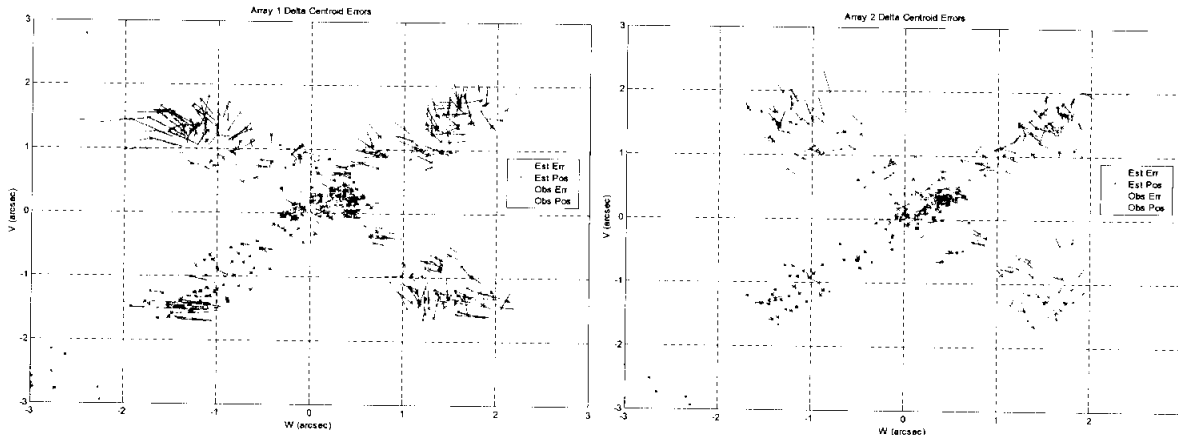


Figure 5: Centroiding errors as a function of position on Arrays 1 and 2.

Since Spitzer's focal surface is shared by all three science instruments plus the PCRS, we needed to verify the optical performance (including confocality and alignment) of the instruments with the flight telescope. Before launch, the PCRS image diameters were measured at Spitzer best focus and at the PCRS best focus, 6.5 arcsec and 2.2 arcsec respectively.⁵ The image size at the nominal Spitzer launch focus, 6.5 arcsec in diameter, falls within our required range of 6 – 8 arcsec. This focus measurement was repeated a number of times post-launch.

Since the PCRS is a visible light sensor, it is not susceptible to changes in the telescope temperature. This makes it the optimal device for tracking the progress of the telescope cooldown after launch. Since the PCRS is operated significantly out of focus, any change in focus results in a simple linear change to the image diameter. Therefore, a measure of the image diameter provides a sensitive measurement of the telescope focus, including its sign. Figure 3 depicts a model of the change in PCRS image diameter with focus. Similarly, PCRS tracked the performance of the telescope on orbit as it cooled from 292 K down to 5.5 K, participating in the SIRTf focus campaigns.⁶ The cooldown

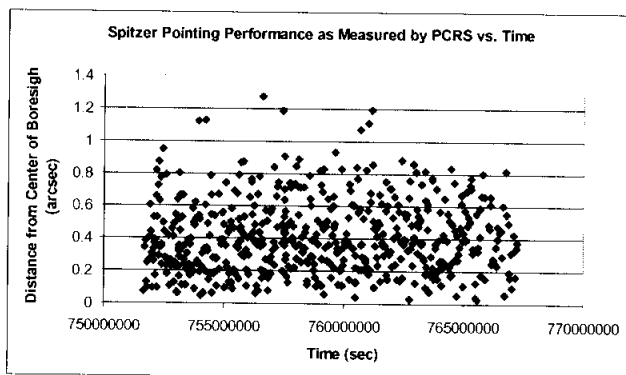


Figure 6: PCRS centroids resulting from S2P calibrations collected over 180 days. The median pointing performance is 0.37 arcsec radial.

resulted in a major focus change in the telescope; by measuring the PCRS' image diameter every two to three days, we successfully tracked the changes in telescope focus in tandem with the IRAC instrument. Figure 4 depicts the change in PCRS image diameter (and therefore focus) as a function of time as the telescope drifted down in temperature and was finally focused by adjusting the secondary mirror.

3.1.6. PSF Calibration

Achieving $<1/20$ pixel centroiding accuracy requires a detailed response map of the PSF to remove systematic errors resulting from a non-uniform PSF. Because the Spitzer telescope was launched warm and changed figures to assume its final shape as it cooled, it was necessary to recalibrate the PCRS PSFs for

Arrays 1 and 2 on-orbit after the telescope equilibrated. This is because the final shape of the flight telescope differed at

the 0.55 μm wavelength used by the PCRS from the telescope simulator built in the laboratory during ground-based testing. About three weeks after launch, we began creating the first PSF calibrations and testing the PCRS centroiding accuracy as the telescope cooled down. The PSF was calibrated by executing a series of very slow radial small-angle slews in gyro-only mode while imaging with the PCRS. Inertial holds were performed after each slew to allow the Observatory's Kalman filter to settle and optimally converge, making for a series of very stable, smooth slews from the center of the array out to +2.5 arcsec in a radial "wagon wheel" pattern. This enabled us to sample the point spread function over a wide range of spatial points for the inner ± 2 arcsec of the four inner pixels (the "sweet spot"). The PCRS observations collected along each outbound leg would have allowed us to create the grid of PSF calibration points to which the Chebyshev polynomials were fitted, but in the end it was deemed more efficacious to use the PCRS observations resulting from the centroiding accuracy tests (described in Section 3.1.7 below) to create the calibration grid. Once the PSF calibration of the inner four pixels was mapped in this way, a set of 20th order Chebyshev polynomials were fitted to the resulting fluxes. These calibration coefficients were uploaded into memory and were used for high accuracy PCRS centroiding.

3.1.7. Centroiding Accuracy

Centroiding accuracy was verified several times before, during, and after PSF calibration for Arrays 1 and 2. Centroiding accuracy was verified by executing a series of precision offset maneuvers using the gyroscopes only. Small

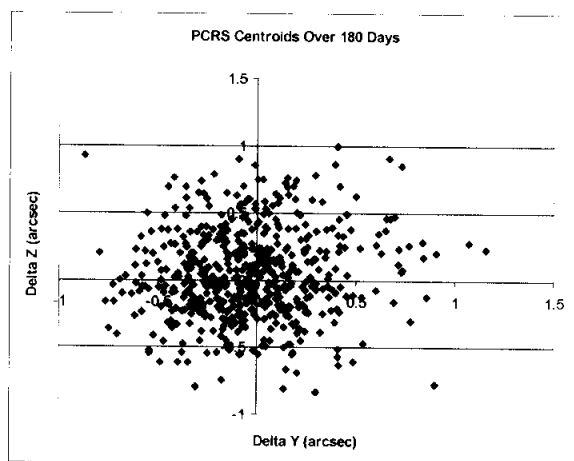


Figure 7: PCRS centroids resulting from S2P calibrations collected over 180 days.

angle offsets can be made extremely precisely using the gyro only. The Observatory's Kalman filter was first stabilized by slewing to the target star then executing an inertial hold for five minutes to allow the filter to converge. Next, a series of boxes with side lengths 1.0, 2.0, 2.6, and 3.0 arcsec were executed, with 100 sec inertial holds at the array center executed between each box. A PCRS observation was collected at each of the box corners and before and after the returns to the array center. Figure 5 shows the results of the several accuracy tests for Arrays 1 and 2. Since Array 2 was focused such that it has a larger image diameter, its behavior is smoother across the inner 2 arcsec, resulting in lower systematic centroiding errors. Nonetheless, both arrays successfully met their centroiding requirements. In this way, 1/100 pixel centroiding was made possible.

3.2. Nominal operations

After the completion of the 60 day in-orbit checkout period, we commenced normal operations with the PCRS primary side. The PCRS is nominally used in two modes: first, to perform twice-daily updates of the telescope boresight location relative to the star trackers and gyros, and second, to initialize precision pointing maneuvers, particularly for the Infrared Spectrograph modules. The star tracker-to-PCRS (S2P) calibration takes out the thermomechanical drift that accumulates between the 5.5 K telescope and the 300 K bus as the Observatory changes orientations in the sunlight. Originally, these calibrations were performed three times daily, but the pointing system appeared so stable that we successfully decreased the interval to one calibration every twelve hours without significant impact to the pointing system. Currently, the overall pointing performance of the Spitzer Space Telescope averages 0.37 arcsec radial 1- σ as measured by the PCRS immediately after an S2P cal. Twelve hours later, at the start of the next S2P calibration, the PCRS measures the overall pointing to be 0.47 arcsec radial 1- σ . Figures 6 and 7 depict an ensemble of PCRS centroids resulting from S2P calibrations over a 180 day period beginning shortly after the final PCRS calibration was complete. This overall pointing accuracy is much better than the required 5 arcsec radial 1- σ .

4. CONCLUSIONS

The PCRS began nominal operations following the August, 2003 launch of the Spitzer Space Telescope and has functioned without failure ever since. We have verified that the PCRS meets all of its centroiding performance requirements in anticipation of the continuation of Spitzer's five year mission.⁷

ACKNOWLEDGEMENTS

A.K.M. gratefully acknowledges Bill Burmester, Joyce Bonar, Angus McMechen, John Schwenker, Jonathan Sievers, John Tietz, Roel VanBezooijen, and Chris Voth for numerous useful contributions. In particular, we thank Daniel Swanson of Lockheed Martin, lead pointing engineer for Spitzer, for his invaluable contributions to the PCRS. The authors would like to thank their family and friends for their inestimable patience and support during the in-orbit checkout of the PCRS, as well as the entire Spitzer team for their dedication, which has led to the mission's unqualified success to date. The work described in this publication was carried out for the Jet Propulsion Laboratory, California Institute of Technology, under a contract with the National Aeronautics and Space Administration.

REFERENCES

1. Mainzer, A. K.; Young, E. T.; Huff, L. W.; Swanon, D.; "Pre-launch performance testing of the pointing calibration and reference sensor for SIRTf." *Proc. SPIE* **4850**, pp. 122M, 2003.
2. Mainzer, Amanda K.; Young, Erick T.; Greene, Thomas P.; Acu, Nagarjuna; Jamieson, Thomas H.; Mora, Hank; Sarfati, Sean; van Bezooijen, Roelof W. "Pointing Calibration and Reference Sensor for the Space Infrared Telescope Facility". *Proc. SPIE* **3356**, pp. 1095-1101, 1998.
3. Young, Erick T.; Davis, James T.; Thompson, Craig L.; Rieke, George H.; Rivlis, G.; Schnurr, Richard; Cadien, James; Davidson, Lacinda; Winters, Gregory S.; Kormos, Karen A. "Far-infrared imaging array for SIRTf". *Proc. SPIE* **3354**, pp. 57-65, 1998.
4. VanBezooijen, R. W. H. "Guide star catalog for the Spitzer Space Telescope pointing calibration and reference sensor". *Proc. SPIE* **5487-95**, 2004.
5. Schwenker, J. P.; Brandl, B. R.; Burmester, W.; Hora, J. L.; Mainzer, A. K.; Quigley, P. C.; VanCleve, J. "SIRTf -CTA optical performance test". *Proc. SPIE* **4850**, pp. 304S, 2003.
6. Gherz, R. D.; Romana, E. A.; Hoffman, W. F.; Schwenker, J. P.; Mentzell, J. E.; Hora, J. L.; Eisenhardt, P. R.; Brandl, B. R.; Armus, L.; Stapelfeldt, K. R.; Hines, D. C.; Mainzer, A. K.; Young, E. T.; Elliot, D. G. "The state of the focus and image quality of the SIRTf CTA." 2003 AAS 203, 2214.
7. Gallagher, David B.; Simmons, Larry L. "Development of the Space Infrared Telescope Facility (SIRTf)". *Proc. SPIE* **4013**, pp. 80-89, 2000.